HIPPOCAMPUS 24:1232–1247 (2014)

Anterior Thalamic Lesions Reduce Spine Density in Both Hippocampal CA1 and Retrosplenial Cortex, but Enrichment Rescues CA1 Spines Only

Bruce C. Harland,[1] David A. Collings,[2] Neil McNaughton,[3] Wickliffe C. Abraham,[3] and John C. Dalrymple-Alford[1,3,4]*

ABSTRACT: Injury to the anterior thalamic nuclei (ATN) may affect both hippocampus and retrosplenial cortex thus explaining some parallels between diencephalic and medial temporal lobe amnesias. We found that standard-housed rats with ATN lesions, compared with standard-housed controls, showed reduced spine density in hippocampal CA1 neurons (basal dendrites, −11.2%; apical dendrites, −9.6%) and in retrospenial granular b cortex (Rgb) neurons (apical dendrites, −20.1%) together with spatial memory deficits on cross maze and radial-arm maze tasks. Additional rats with ATN lesions were also shown to display a severe deficit on spatial working memory in the cross-maze, but subsequent enriched housing ameliorated their performance on both this task and the radial-arm maze. These enriched rats with ATN lesions also showed recovery of both basal and apical CA1 spine density to levels comparable to that of the standard-housed controls, but no recovery of Rgb spine density. Inspection of spine types in the CA1 neurons showed that ATN lesions reduced the density of thin spines and mushroom spines, but not stubby spines; while enrichment promoted recovery of thin spines. Comparison with enriched rats that received pseudo-training, which provided comparable task-related experience, but no explicit spatial memory training, suggested that basal CA1 spine density in particular was associated with spatial learning and memory performance. Distal pathology in terms of reduced integrity of hippocampal and retrosplenial microstructure provides clear support for the influence of the ATN lesions on the extended hippocampal system. The reversal by postoperative enrichment of this deficit in the hippocampus but not the retrosplenial cortex may indicate region-specific mechanisms of recovery after ATN injury. © 2014 Wiley Periodicals, Inc.

KEY WORDS: spatial memory; environmental enrichment; neuromorphology; hippocampus; retrosplenial granular b cortex

INTRODUCTION

The anterior thalamic nuclei (ATN) are part of a distributed network associated with episodic memory. Damage to, or disconnection of, this region is evident in clinical conditions presenting with severe anterograde amnesia, such as thalamic stroke or Korsakoff's syndrome (Harding et al., 2000; van der Werf et al., 2002; Carlesimo et al., 2011). The pattern of memory deficits after ATN lesions in rats is often comparable to that caused by hippocampal system lesions (Mitchell and Dalrymple-Alford, 2006; Wolff et al., 2006; Sziklas and Petrides, 2007; Aggleton, 2008; Moreau et al., 2012; Dumont and Aggleton, 2013), leading to growing recognition that the ATN are a key point of convergence of an extended hippocampal system (Aggleton and Brown, 2006; Aggleton et al., 2010). Interdependence of the ATN and the hippocampal formation is reinforced by crossed-lesion studies in which contralateral lesions produced spatial memory impairments when ipsilateral did not (Warburton et al., 2001; Henry et al., 2004). Similarly, lesions to hippocampus, ATN, mammillothalamic tract, or Gudden's ventral tegmental nuclei substantially reduce expression in the retrosplenial cortex of immediate early gene (IEG) markers. This common retrosplenial effect suggests that these brain regions function together to support memory (Jenkins et al., 2002a,b; Aggleton, 2008; Vann and Albasser, 2009; Vann, 2013).

A new proposal that has received relatively little attention is the idea that the ATN primarily influence the hippocampus rather than vice versa (Vann, 2010; Aggleton et al., 2010). If so, ATN injury should negatively affect the hippocampus, despite the connections being indirect via the subicular complex and retrosplenial cortex (Shibata, 1993). Functional changes in the hippocampus after ATN lesions have been reported, such as reduced phosphorylated CREB (pCREB) and IEG markers (c-Fos; *zif268*), but these are generally weaker compared with changes in the retrosplenial cortex and not always found in the case of IEG markers (Jenkins et al., 2002a,b; Dumont et al., 2012; Dupire et al., 2013). We reasoned that ATN lesions should have robust effects on the hippocampus, so we

[1] **Department of Psychology, University of Canterbury, Christchurch, New Zealand;** [2] **School of Biological Sciences, University of Canterbury, Christchurch, New Zealand;** [3] **Department of Psychology and Brain Health Research Centre, University of Otago, Dunedin, New Zealand;** [4] **New Zealand Brain Research Institute, Christchurch, New Zealand**

Grant sponsors: Health Research Council of New Zealand International Investment Opportunities Fund; Grant number: 09/051; Neurological Foundation of New Zealand; University of Canterbury, New Zealand.

*Correspondence to: John C. Dalrymple-Alford, New Zealand Brain Research Institute, and Department of Psychology, University of Canterbury, Private Bag 4800, Christchurch, New Zealand.
E-mail: john.dalrymple-alford@canterbury.ac.nz

Accepted for publication 22 May 2014.
DOI 10.1002/hipo.22309
Published online 26 May 2014 in Wiley Online Library (wileyonlinelibrary.com).

examined whether these lesions influenced hippocampal microstructure integrity. CA1 spine density was selected because this sub-region may have more influence on the extended hippocampal system. The CA1 is a primary source of hippocampal outputs, with collateral projections to multiple brain regions (Cenquizca and Swanson, 2006; Aggleton, 2012).

By comparison with the hippocampus, ATN lesions strongly and consistently reduce IEG in the retrosplenial cortex, a region associated with the integration of egocentric and allocentric spatial information (Poirier and Aggleton, 2009; Pothuizen et al., 2010). The most dramatic c-Fos reductions are found in the superficial layers of the retrosplenial granular b cortex (Rgb), which receive dense thalamocortical projections from all three ATN subdivisions (Shibata, 1993; Aggleton, 2008). These reductions in IEG markers indicate alterations in plasticity and metabolism, but ATN lesions do not alter the appearance of the retrosplenial cortex when assessed by standard histological techniques such as the number and density of Nissl stained cells. As a consequence, reduced IEG expression in the retrosplenial cortex has been described as "covert pathology" (Aggleton, 2008). In view of these interesting findings, the current study examined whether ATN lesions result in reduced microstructural complexity at the level of spine density in the superficial layers of the Rgb.

Recovery of spatial memory is evident in rats with ATN lesions when they are housed postoperatively in an enriched environment. Restoration of the flexible use of spatial reference memory has been demonstrated (Wolff et al., 2008), as well as improved spatial working memory even after deficits have been established and enrichment introduced only 40 days postlesion (Loukavenko et al., 2007). We postulated that recovery of spatial memory performance observed in enriched rats with ATN lesions may represent a reversal of any lesion-induced microstructural changes in the hippocampus and retrosplenial cortex. Support for this idea comes from evidence that enrichment ameliorated reduced CA1 spine density after subicular lesions (Bindu et al., 2007), but would be more convincing in our case because the ATN, unlike the subiculum, does not have direct connections with CA1. The ATN have direct connections with the retrosplenial cortex, so the effects of ATN lesions and recovery might be expected to be stronger in the retrosplenial cortex than in the CA1 region. These objectives were addressed by evaluating spine density in CA1 and Rgb neurons in ATN and sham-lesion rats that were housed in either standard or enriched cages.

Additional enriched-housed sham and ATN-lesion groups were given pseudo-training. Pseudo-training provided comparable task-related experience to that of formal spatial memory training. Increased spine density with formal training would suggest an influence of spatial learning and memory beyond general behavioural testing. Pseudo-training controls have not been used to examine CA1 spines or Rgb spines and hippocampus-dependent spatial memory, although a similar contrast demonstrated increased CA1 apical, but not basal, spines after acquisition of an olfactory discrimination task (Knafo et al., 2004). The influence of pseudo-training has not been examined in enriched rats. The previous link between basal CA1 spines and spatial memory was established using trained enriched rats compared with non-trained single or pair-housed rats (Moser et al., 1994, 1997).

MATERIALS AND METHODS

Animals, Surgery, and Experimental Groups

Eighty PVG male hooded rats were used (8–10 months old, between 366 and 456 g at surgery; for final *n*, see lesion analysis). The rats were maintained in reversed 12-h light schedule (8 a.m. to 8 p.m.) in their colony room so that all behavioural testing was conducted during the dark phase when activity levels are higher. Aspects of the circadian cycle may have been altered by this testing regime, but observation of the rats in their home cage confirmed that in the colony room high home cage activity was maintained when lights were off and low home cage activity maintained when lights were on. Similar memory deficits have been reported after ATN lesions irrespective of light cycle and time of day of testing (Loukavenko et al., 2007; Dumont et al., 2012; Dupire et al., 2013). Body weights were restricted to 85 to 90% of free-feeding weight during testing, with free food access for surgery, recovery, and during subsequent 40-day continuous enrichment period. All protocols in this study conformed to the NIH Guide for the Care and Use of Laboratory Animals and were approved by the Animal Ethics Committee, University of Canterbury.

All rats were housed in groups of three or four per standard plastic cage (50 cm × 30 cm × 23 cm high) before surgery. Based on preoperative spatial working memory performance in a cross-maze, matched pairs of rats were randomly assigned to either the anterior thalamic nuclei (AT) or sham (SH) lesion condition. Rats were anesthetized intraperitoneally with ketamine (70 mg/kg) and domitor (0.5 mg/kg) and placed in a stereotaxic frame with atraumatic ear bars (Kopf, Tujunga, CA) and the incisor bar −7.5 mm below the interaural line. Two infusion sites in each hemisphere were directed at the anteroventral nucleus (AV), followed by a single infusion in each hemisphere directed at the anteromedial nucleus (AM). Each surgery used one of five anterior–posterior coordinates relative to an individual rat's bregma to lambda (B–L) distance. For the AV lesions, the AP coordinates from bregma were: −2.4 for B-L ≤ 6.4; −2.45 for B-L = 6.5 to 6.8; −2.5 for B-L = 6.9 to 7.2; −2.55 for B-L ≥ 7.3. The AV infusions were made at ventrality −5.63 mm followed by −5.73 from dura at ±1.52 mm lateral to the midline. The AM infusion was placed 0.1 mm more anterior than the for the AV sites, with laterality ±1.20 mm and ventrality −5.86 mm. A microinfusion pump (Stoelting, Reno, NV) delivered either 0.16 μl (each of the two AV sites per hemisphere) or 0.20 μl (single AM site) of 0.15 M *N*-methyl-D-aspartic acid (NMDA; Sigma, Castle Hill, NSW, Australia) in phosphate buffer (pH 7.2) at 0.04 μl/min using a 1-μl Hamilton syringe. The needle was left in situ at

each site for 3 min postinfusion. For SH the needle was lowered to 1.50 mm above lesion coordinates without infusion.

The main aim of the experiment was to compare the effects of standard groups housing (Std) versus enriched housing (Enr) across sham lesion (SH) and AT lesion groups. This aim was addressed using four groups of rats that received formal spatial memory training (Tr) throughout the experiment: sham standard-housed trained (SH-Std-Tr); sham enriched trained (SH-Enr-Tr); AT standard-housed trained (AT-Std-Tr); AT enriched trained (AT-Enr-Tr). An additional two groups of enriched rats were used that received pseudo-training procedures that were introduced only after the period of postoperative enrichment (sham enriched pseudo-trained, SH-Enr-Ps; and AT enriched pseudo-trained, AT-Enr-Ps). The pseudo-training groups enabled a comparison of the neuroanatomical effects of the formal spatial memory training procedures as opposed to exposure to general training procedures after the period of enrichment. To ensure similar early experience, all six groups of rats received training in a cross-maze both before surgery (the first period of formal training on that task) and after surgery before enrichment (the second period of formal training on that task). This second period of cross-maze testing was conducted two to three weeks postsurgery to establish the effects of ATN lesions and sham lesions on spatial working memory. Rats with similar rank-ordered scores that were obtained during this postoperative test were randomly allocated across groups to match levels of postoperative performance between the future standard-housed and enriched rats (within each surgery condition) before placement in the different housing conditions. This procedure ensured that deficits after ATN lesions had been established before the housing manipulations.

After the 40-day continuous enrichment (or matched standard housing) period, the four main groups (Tr) were retested on the cross-maze task (i.e. their third period of formal testing on that task), before being given formal training for the first time on a new spatial memory task, the radial-arm maze. The radial-arm maze task assessed the generality and persistence of spatial memory effects of lesion and enrichment before neuroanatomical analysis. By contrast, the SH-Enr-Ps and AT-Enr-Ps groups now only received pseudo-training procedures, after the enrichment period, so that they continued to experience similar exposure to the general test conditions as rats in the Tr groups, but no subsequent formal spatial memory training. That is, these pseudo-training groups received the behavioural control procedures during the final period of cross maze testing and during radial arm maze testing.

Housing

All rats were housed individually for 7 to 11 days to allow recovery from surgery and then were re-caged in groups of three or four for postsurgery cross-maze testing. Rats then received 40 days of continuous housing in either an enriched environment or standard caging during which no behavioral testing occurred. Rats that continued with standard caging were housed with new cage-mates. Both types of housing included both AT and SH rats within each cage. Rats in the enriched environments were housed with 11 or 12 new cage-mates in a large wire-mesh cage (85 cm $\times$ 60 cm $\times$ 30 cm high) with all the enrichment objects and the position of food and water changed daily using a standardized arrangement of objects that differed every day throughout the enrichment period (see http://www.psyc.canterbury.ac.nz/StandardizedEnrichment.shtml). Thirteen objects were introduced each day, no single object was repeated within 5 days, and 1 day with no enrichment objects was programmed every eighth day. Placement of the enrichment cages within the colony room was changed every fourth day. After 40 days of these different housing conditions, the enriched groups were re-housed in groups of three or four in standard conditions with cage-mates from the same enriched environment cage during the day and enrichment at night ($\sim$6 p.m. to $\sim$10 a.m.) for the remainder of the experiment. This procedure facilitated behavioural testing and the provision of the daily food ration after testing ($\sim$5 p.m.) when all rats were in standard cages.

Cross-Maze Task

Spatial working memory was tested using a T-maze configuration embedded in a cross-maze raised 75 cm above the floor. This task provided a sensitive behavioural assay for spatial memory deficits produced by ATN lesions (Aggleton and Brown, 1999; Loukavenko et al., 2007). The same apparatus, room, and distal cues were used for presurgery, postsurgery, and postenrichment cross-maze testing. The wooden runways were 10.5 cm wide and painted gray, with 2.5 cm high galvanized steel borders. The two stems were 1 m long with a guillotine door located 28 cm from each end to create the two start areas (labeled S and N) and flanked by clear Perspex barriers (10 cm wide by 25 cm high). The two 40 cm long goal arms (labeled A and B) each had a raised wooden food well (2.5 cm diameter, and 1 cm deep) holding inaccessible food rewards to provide constant olfactory cues. Wooden blocks (10.5 cm wide by 30 cm high by 10 cm deep) were used to restrict access to any stem or arm. The maze was located diagonally in a windowless room (334 cm by 322 cm) which provided a rich source of distal cues. Beyond one goal arm was a computer monitor on a small table, while a folded-back curtain and empty corner faced the other arm; beyond one start area was a closed door embedded in a small alcove and a hub from a radial-arm maze was beyond the other start area. Three sets of three or four three-dimensional objects were attached to the walls in different locations, configurations, and heights. The horizontal distance between the maze and the nearest surface varied from 30 cm to 80 cm. Diffuse lighting was provided by overhead fluorescent lights. The rats were familiarized to the maze preoperatively over a week with 0.1 g chocolate pieces scattered on the maze that were progressively reduced until they were found only at the food wells. At the start of postsurgery and postenrichment testing the rats were given 1 day of pretraining to re-familiarize them with the maze using pseudo-random forced-choice runs only.

Before surgery, rats were trained to criterion (87.5% accuracy over four consecutive sessions) for a minimum of 15 and maximum of 32 sessions. They were retested for 10 sessions at 2 to 3 weeks postsurgery and for another 10 sessions at 1 week postenrichment. Six trials were conducted per session throughout testing, with each trial consisting of a sample and test run with a ~5 s intra-trial delay in the start area. In the sample run, the rat was placed in one of the start areas for 8 s before the door was lifted and an arm block forced it to enter either the left or right goal arm on a pseudo-random basis (Fellow, 1967) for a reward of a 0.1 g chocolate piece. In the test run, the rats were held in one of the two start areas for 8 s again before being allowed a choice of either goal arm (neither arm was blocked), but was only rewarded (with 0.2 g of chocolate) for entering the goal arm that was not visited in the sample run. For both sample and test runs, once a rat entered a goal-arm it was given 10 s to eat the chocolate and/or look around; if an error occurred, the rat was retained in that arm for 10 s. The rat was returned to the home cage in the testing room between trials until all its cage-mates had received their trial, resulting in an inter-trial interval of about 3 to 4 min. Pseudo-randomly for half of the sample runs per session, the rat was initially held in start area *S*, and for the other half it was placed in start area *N*. For the test run on half of the trials and balanced across start area the rats were also pseudo-randomly placed in either the same start area for a "same start" test run or in the opposite start area for an "opposite start" test run. This procedure prevented the task being solved using a simple egocentric strategy, because alternate body turns on test runs are feasible if the rat always starts from the same start area on both sample and test runs.

All rats received the above training regime before surgery and at 2 to 3 weeks postsurgery. After the enrichment period, however, the two enriched-housed pseudo-trained groups received a different cross-maze test procedure to the other four groups that received regular spatial memory training. SH-Enr-Ps rats received similar runs and rewards to some of the SH-Enr-Tr rats and AT-Enr-Ps rats received similar runs and rewards to some of the AT-Enr-Tr rats, receiving each of their cross-maze trials immediately after that yoked rat. The sample runs for the pseudo-trained rats were identical to the trained rat's sample run, but instead of a regular test run the rat received a second forced choice run (pseudo-test run) which, for any given day, was pseudo-randomly "always left" for that day or "always right" for that day. The start areas used on the pseudo-sample and pseudo-test runs were yoked to those used for the trained rats. The pseudo-trained rats were rewarded with one chocolate piece for both runs to ensure they ran consistently while receiving a comparable number of rewards to trained rats (i.e. 12 pieces vs. a minimum of 6 and maximum of 18 in the trained rats).

Radial-Arm Maze Task

This task provided evidence on the acquisition of a new task and spatial environment. One or 2 days after postenrichment cross-maze testing, rats received 4 days of familiarization and pretraining in an 8-arm radial maze. They were first placed with cage-mates on the maze with numerous chocolate pieces scattered on the maze and then individual rats were familiarized with the maze's doors and to search for chocolate pieces in the food wells. The maze was raised 67.5 cm above the floor and was constructed of a 35 cm wide black wooden hub with eight detachable aluminum arms (65 cm long by 8.6 cm wide, 3.9 cm-high borders). Single clear Perspex barriers (19 cm × 25 cm) extended along each arm from the central hub to discourage rats from jumping across arms. A black wooden block (5 cm long × 8.5 cm wide × 3 cm high) provided a food well (2 cm diameter, 1 cm deep) at the end of each arm and housed inaccessible food (0.1 g chocolate pieces) to provide constant olfactory cues. Clear Perspex guillotine doors (4.5 cm wide × 2.5 cm high) controlled access to the arms and could be raised singly or together by an overhead pulley system. The radial maze was close to one corner of a different windowless room to that used for the cross-maze and this room also contained several distal cues. Near one corner was a small stand with three large objects (large brown cup, white plastic spouting, and a large black ceramic ball), with a drawn ceiling-mounted curtain nearby. Various large pieces of a Perspex maze were located on the other side of the room. The experimenter sat at a large table with a computer monitor linked to a ceiling-mounted camera above the maze. This table held a pulley system by which the experimenter lifted either a single door or all doors simultaneously. Behind the experimenter was a sink, cupboard and several stacked trays filled with sand. A trolley containing testing cages was adjacent to the room's door. The radial-arm maze arms were 50 cm to 115 cm distant from any item in the room. This testing room had the same level of diffuse lighting as the room used for cross-maze testing.

For each session, seven of the arms were baited with two pieces of chocolate each (0.2 g of chocolate at each food-well) and one arm was never baited (pseudo-randomly varied across rats) to increase the spatial demands of the task. Arms were pseudo-randomly repositioned at the start of each day's testing so that the unbaited arm for each rat represented a fixed location in the room. In any session the rat was removed once all seven chocolate rewards were claimed or allowed a maximum of 20 arm visits or 10 minutes in the maze. At the start of the session the rat was placed in the central hub for a 5 s delay before all the doors were simultaneously lifted. Once the rat entered an arm, all other doors were closed while the rat ran to the food well and then returned to the central hub, followed by closing that door and another 5 s delay. Testing sessions were conducted on consecutive days for 7 days a week. The task was run for a minimum of 15 days and a maximum of 35 days or until the rat reached a criterion of two out of three sessions without visiting the unbaited arm and had made no more than five working memory errors in total over the three sessions. Rats failing to reach criterion were given a score of 35 + 3 "criterion" days.

The two enriched-housed pseudo-trained groups again received a different procedure to those that received spatial memory training. Each pseudo-trained rat was pseudo-randomly

designated a single arm location (not a physical maze arm) so that these arm locations were evenly distributed amongst the pseudo-trained rats. At the start of the session the rat was placed in the central hub but after the 5 s delay only the door to the rat's designated arm was opened. Pseudo-trained rats were allowed 10 visits to their designated arm, with a 5 s delay in the central hub between visits during which the arm was re-baited. Over the 10 visits the pseudo-trained rats received a total of 15 chocolate pieces, comparable to the 14 pieces that trained rats would receive for visiting all of their baited arms. SH-Enr-Ps rats were randomly selected to be sacrificed around the same time as SH-Enr-Tr rats reached the criterion. SH-Enr-Tr rats took an average of 21.9 (±SD 6.7) days to reach criterion, and the SH-Enr-Ps rats received an average of 20.1 (±SD 5.1) days to of pseudo-training ($t < 1.0$). AT-Enr-Ps rats received the same duration of radial-arm maze pseudo-training as an AT-Enr-Tr rat that appeared to perform similarly during the previous postsurgery cross-maze test. After confirmation of accurate lesions (see Lesion Evaluation) the AT-Enr-Tr group took an average of 27.6 (±SD 6.1) days to reach criterion and the AT-Enr-Ps group had received an average of 26.3 (±SD 5.1) days of pseudo-training ($t < 1.0$).

Anatomical Methods

The rats were given an overdose of sodium pentobarbital 24 h after either reaching criterion or the maximum number of days of testing (35 days) in the radial-arm maze task. The brains were removed fresh and rinsed with Milli-Q water before being cut into slabs using a brain matrix (Ted Pella, Kitchener, Canada). A 3-mm thick slab of brain encompassing the anterior thalamic region was postfixed in 4% 0.1 M paraformaldehyde and cut into 50 μm coronal sections using a vibratome (Campden Instruments, London, United Kingdom). Cresyl violet staining was used to evaluate the thalamic lesions by an experimenter blinded to group status and behavioural data. The lesion areas were drawn on electronic copies of the Paxinos and Watson (1998) rat brain atlas so that automated pixel counts of the damaged regions could be used to estimate lesion volumes by factoring in the distances provided by the atlas (Mitchell and Dalrymple-Alford, 2006). Collapse of areas surrounding the ATN and adjacent thalamic region and variability in angle of sections required a conventional visual, rather than direct image, analysis.

Golgi stain (FD NeuroTechnologies, Columbia, MD) was used to visualize neurons in 200 μm coronal sections cut from a 4 mm slab containing the dorsal hippocampus and retrosplenial granular b cortex. Dendrites on CA1 and Rgb cells were selected from slides that had been re-coded by a researcher not involved in the study to ensure blinded evaluations. To account for variation in spine density across neurons and across segments a large total number of dendritic segments (between 20 μm and 25 μm in length) were included in the analysis (CA1 basal = 944; CA1 apical = 861; Rgb apical = 390) resulting in the identification of a large number of dendritic spines (CA1 basal = 41,556; CA1 apical = 39,392; Rgb apical = 11,116).

For CA1 dendritic spine analysis, a Leica laser scanning confocal microscope (Leica model SP5, Wetzlar, Germany) was used to image 7 to 18 basal dendritic segments (mean = 15.23, SD = 3.02) and 6 to 18 apical dendritic segments (mean = 13.89, SD = 3.39) per rat that were selected from pyramidal neurons in the dorsal CA1 (generally the middle of CA1 in the medial to lateral orientation). A 63× NA 1.3 glycerol-immersion objective was used to collect high-resolution transmitted light image stacks. An argon laser (488 nm) running at 20% power was used to collect 2,048 × 2,048 pixel images which, with 2× digital zoom, gave a resolution of 60 nm per pixel. Optical series were collected with a 0.2 μm step size and with 40 to 60 images per stack. Basal segments for spine density analysis were taken from tertiary or quarternary branches in the stratum oriens that were at least 50 μm from the cell body (see Results). Apical segments were taken from lateral oblique dendrites in the stratum radiatum emerging from a primary apical trunk at least 150 μm from the cell body and before the stratum lacunosum-moleculare.

For Rgb apical spine analysis in cell layer I, a Zeiss microscope (Axio Imager M1, Göttingen, Germany) was used to image 6 to 7 apical dendritic segments per rat that were selected from layer II/III fusiform pyramidal neurons in the Rgb. A 100× NA 1.3 oil-immersion objective was used to collect high resolution transmitted light image stacks consisting of 3,900 × 3,090 pixel images which gave a resolution of 56 nm per pixel. Optical series were collected with a 0.2 μm step size and with 40 to 60 images per stack. Apical segments were taken from dendrites in cell layer I that were not part of the primary apical trunk and were at least 50 μm from the cell body (see Results).

All dendritic segments from CA1 and Rgb neurons were between 20 μm and 25 μm in length, had to be in one focal plane and located near the top surface of the section, unobscured by artefacts or other dendrites, and commence at least 10 μm from any branching points or terminals. Dendritic segments were reconstructed from image stacks and traced over a two year period using Neurolucida (MicroBrightField Bioscience) by a single experimenter (BH). Spines were classified as "thin" or "mushroom" or "stubby" using a classification system adapted from Harris et al. (1992) and De Simoni et al. (2003). Spines were designated as "thin" if the length of the spine was greater than the neck diameter and the neck diameter was less than three times the diameter of the spine head. 'Mushroom" spines were identified if the diameter of the head was at least three times as wide as the diameter of the neck. "Stubby" spines had a base neck diameter that was equal or larger than the total length of the spine. No attempt was made to introduce a correction factor for hidden spines (above or below the field of view) during the spine labeling and classification process.

Statistical Analyses

The primary aim of the study was to examine the effects of Lesion surgery (SH, AT) and Housing (Standard, Enriched) in

the four trained groups (SH-Std-Tr, AT-Std-Tr, SH-Enr-Tr, AT-Enr-Tr). This aim was assessed using a 2 × 2 analysis of variance. Analysis of postsurgery and postenrichment cross-maze performance added the factors Session (1–10) and Trial Type (Same Start, Opposite Start). As in previous work, the last three sessions (when overall performance was relatively stable) of both the postsurgery and postenrichment cross-maze tests were examined more closely to assess the effects of ATN lesions with respect to trial type (Loukavenko et al., 2007). Radial-arm maze performance was scored on days to reach criterion. The average number of baited and unbaited spatial working memory errors in the radial-arm maze were also analysed separately by adding the factor Blocks (seven blocks of 5 days). Similarly, 2 × 2 ANOVA (Lesion: Sham, AT; Housing: Standard, Enriched) examined spine density in the four trained groups of rats, using values averaged across spine segments within-animal. Total spine density was analysed separately for basal and apical dendritic CA1 segments and apical dendritic Rgb segments, followed by analyses restricted to thin, mushroom, and stubby spines. Supplementary ANOVA then assessed spine density in the four enriched groups with respect to SH versus AT surgery and Training versus Pseudo-training (SH-Enr-Tr, AT-Enr-Tr, SH-Enr-Ps, AT-Enr-Ps); note that this supplementary analysis shared the same enriched trained groups as was used in the primary analyses (SH-Enr-Tr and AT-Enr-Tr). Where relevant, effect sizes between conditions or groups were expressed as Cohen's *d*.

To account for the potential confounds of variation in the dendritic segments examined, the spine analyses were repeated with the number of dendritic segments analysed per rat and the average diameter of dendritic segments per rat as covariates. Neither covariate was significant for the CA1 basal or apical segments ($F < 3.0$) or the Rgb apical segments ($F < 3.5$), and none of the conclusions derived from the original analyses reported below were changed by the inclusion of these covariates. For the CA1 dendritic segments, the same results were also found when the analyses were repeated using only segments obtained from rats that provided both tertiary and quarternary branches (Branch Type, relevant to basal segments only, $N = 55$), segments from both anterodorsal and posterodorsal CA1 cells (Location: basal $N = 47$; apical $N = 47$) and segments from both left and right hemisphere (basal $N = 54$, apical $N = 48$), and there were no significant main effects related to any of these three additional factors. Similarly, for the Rgb dendritic segments the conclusions were unchanged when the analyses were repeated using only rats with segments obtained from both the left and right hemisphere.

Given that the treatments affected CA1 and Rgb spines, stepwise regression was used to determine the capacity of spine measures to predict baited arm errors in the radial-arm maze, the behavioural task that was proximal to sacrifice. Any variables omitted by the stepwise procedure were then forced into the equation to determine their relationships with behaviour and the previously extracted variables. Additional stepwise regressions were carried out with the inclusion of Lesion and Housing variables to determine to what extent the observed spine relationships were controlled by these factors.

RESULTS

Lesion Evaluation

The locations of the largest and smallest lesions are shown in Figure 1. As in previous studies, only rats with lesions that encompassed 50% or more of the ATN and less than 40% damage to the adjacent dorsal medial (MT) and lateral (LT) thalamic nuclei were included for analysis (see Mitchell and Dalrymple-Alford, 2006). Lesion failures occurred in 18 rats, which were not processed further (14 had minor ATN damage; 2 had unilateral lesions; 1 had greater than 40% damage to adjacent lateral thalamic region; 1 had fornix damage). The final sample sizes were: $n = 10$ SH-Std-Tr; $n = 14$ SH-Enr-Tr; $n = 12$ AT-Std-Tr; $n = 9$ AT-Enr-Tr; $n = 9$ SH-Enr-Ps; and $n = 8$ AT-Enr-Ps. Mean lesion volumes for three AT groups are shown in Table 1 as a percentage of damage per region. The paraventricular plus posterior paraventricular nucleus was intact in all three AT groups. There was no difference in ATN lesion volume across the three AT groups ($F < 1.0$). As in previous studies, cresyl violet staining showed apparently normal cellular appearance in all other brain regions after lesions, including the retrosplenial cortex (Jenkins et al., 2004).

Cross-Maze Task

Postsurgery cross-maze testing confirmed that ATN lesions produced the expected severe spatial working memory deficits (Lesion, $F_{(1,41)} = 38.26$, $P < 0.001$; $d = 2.40$, 95% CI 1.80–3.00; Fig. 2A). The matching procedure produced two groups of rats with ATN lesions that showed equally severe impairments in postsurgery testing, before different housing conditions (Housing main effect and Lesion × Housing, $F < 1.0$). At this point, the AT groups showed relatively little improvement across sessions whereas the sham groups reacquired the task rapidly (Lesion by Session, $F_{(9,369)} = 2.35$, $P < 0.02$). There was also a main effect for Trial Type, with rats experiencing far greater difficulty in solving the working memory task when the "opposite start position" was used on the test run (e.g. when *N* was used for sample and *S* for test run for a trial) than when the "same start position" (e.g. *N* for both) was used for both runs ($F_{(1,41)} = 30.96$, $P < 0.001$). There was no interaction between Trial Type and other factors ($F < 1.1$).

As in previous studies, we examined the trial type effect more closely for the last three sessions of postsurgery testing (Fig. 2B). The highly significant Lesion effect remained ($F_{(1,41)} = 37.86$, $P < 0.001$), again with no Housing effect or Lesion × Housing interaction ($F < 2.3$). There was a significant trial type effect ($F_{(1,41)} = 23.27$, $P < 0.001$), but no interactions between Trial Type and any other factor (all $F < 2.5$). Nonetheless, characterizing each group's performance relative to chance (50%) using one-sample t-tests suggested subtle differences across the four groups. Specifically, both the (future) AT-Enr-Tr and AT-Std-Tr groups were significantly above 50% chance on the "same start position" trials ($t_{(8)} = 4.36$, $P < 0.01$, and $t_{(11)} = 3.42$, $P < 0.01$, respectively), but were at

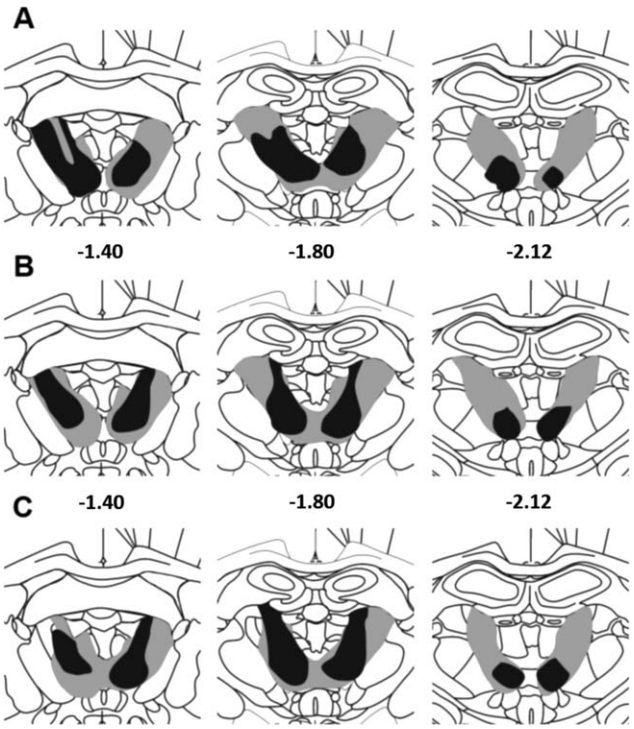

FIGURE 1. Coronal schematics through the medial thalamus showing area of cell loss in the smallest (black) and largest (gray) ATN lesions in A) AT-Std-Tr, B) AT-Enr-Tr, and C) AT-Enr-Ps groups. Values indicate distance from bregma in millimetres (plates adapted from Paxinos and Watson, 1998).

chance levels on the "opposite start position" trials ($t_{(8)} = 0.34$, $P > 0.7$, and $t_{(11)} = -0.30$, $P > 0.7$, respectively). The SH-Enr-Tr and SH-Std-Tr groups scored well above chance on both the "same start position" trials, ($t_{(13)} = 11.32$, $P < 0.001$, and $t_{(9)} = 16.41$, $P < 0.001$) and the "opposite start position" trials, ($t_{(13)} = 4.63$, $P < 0.001$, and $t_{(9)} = 4.99$, $P < 0.001$).

Postenrichment, the cross-maze testing showed that severe deficits continued in rats with ATN lesions (Lesion, $F_{(1,41)} = 20.10$, $P < 0.001$; $d = 1.82$, CI 1.22–2.42), but there was now also a Housing effect ($F_{(1,41)} = 6.67$, $P < 0.02$; $d = 0.83$, CI 0.23–1.42), confirming that rats housed in enriched environments performed better than the standard-housed rats, irrespective of lesion (Lesion × Housing, $F < 1.0$; Fig. 2C). Post hoc Newman-Keuls tests examined the performance of the groups aggregated across the ten sessions. The AT-Enr-Tr group achieved higher performance than the AT-Std-Tr group ($P < 0.02$). While the AT-Enr-Tr group achieved lower percent correct scores than the SH-Enr-Tr group ($P < 0.05$), it was not significantly different to the SH-Std-Tr group ($P > 0.15$). As before, rats performed better when the "same start position" trials were used than when the "opposite start position" trials were used (Trial Type, $F_{(1,41)} = 32.31$, $P < 0.001$).

For the last three sessions postenrichment, when trial type effects were again examined more closely, there was a Lesion effect ($F_{(1,41)} = 9.00$, $P < 0.01$; $d = 1.07$, CI 0.48–1.67) and Housing effect ($F_{(1,41)} = 7.89$, $P < 0.01$; $d = 0.92$, CI 0.32–1.51) but no Lesion × Housing interaction ($F < 1.0$; Fig. 2D). There was a significant Trial Type effect ($F_{(1,41)} = 5.94$, $P < 0.02$), but no interactions between Trial Type and any other factor ($F < 1.0$). Characterizing each group's performance relative to chance (50%) for these last three postenrichment sessions, both sham groups were again significantly above chance for both trial types ($t > 6.0$, $P < 0.002$). As previously, the AT-Std-Tr group performed above chance for the "same start position" trials ($t_{(11)} = 3.34$, $P < 0.01$), but remained at chance ($t_{(11)} = 1.41$, $P = 0.19$) on the "opposite start position" trials. By contrast, the AT-Enr-Tr group now showed clear evidence of improvement, performing significantly above chance for both the "same start position" trials ($t_{(8)} = 3.64$, $P < 0.01$) and the more difficult "opposite start position" trials ($t_{(8)} = 3.35$, $P < 0.02$).

Radial-Arm Maze Task

ATN lesions produced severe deficits in standard-housed rats whereas enrichment of rats with ATN lesions substantially reduced this impairment. Only one rat in each of the two sham groups and two rats in the AT-Enr-Tr group failed to reach criterion in the maximum number of 35 days of testing. By contrast, all of the rats in the AT-Std-Tr group failed to reach criterion (Fig. 2E). For days to

TABLE 1.

Mean Percentage (± SD) of Bilateral Damage to the ATN, Adjacent Medial Thalamic Aggregates and Nuclei

Region	ATN	MT	LT	IAM	LD	PT	PVA	Re	Rh
Group									
AT-Std-Tr, $n = 12$	74.8 (14.5)	1.1 (1.5)	10.8 (9.9)	46.5 (14.9)	3.4 (4.2)	18.0 (10.4)	0.5 (1.6)	3.1 (4.5)	5.6 (8.2)
AT-Enr-Tr, $n = 9$	75.1 (14.7)	2.3 (4.2)	13.9 (12.1)	46.2 (14.2)	2.9 (3.5)	14.1 (6.3)	0.0 (0.1)	1.4 (1.0)	2.4 (4.1)
AT-Enr-Ps, $n = 8$	78.6 (11.3)	0.8 (0.7)	13.0 (7.7)	48.8 (12.9)	2.9 (3.6)	15.3 (7.3)	0.0 (0.1)	1.7 (2.0)	4.4 (5.0)

Mean percentage (± SD) of damage to the medial thalamus in the three ATN lesion groups.
ATN = anterior thalamic nuclei aggregate comprising the anterodorsal, anteromedial and anteroventral thalamic nuclei; MT = posteromedial thalamic aggregate comprising the central and medial mediodorsal nuclei and the intermediodorsal nucleus; LT = lateral medial thalamic aggregate comprising the intralaminar nuclei (centrolateral, paracentral and rostral central medial nuclei) and lateral mediodorsal thalamic nuclei (lateral and paralamellar nuclei); IAM = interanterodorsal nucleus; LD = laterodorsal nucleus; PT = paratenial nucleus; PVA = anterior paraventricular nucleus; Re = reuniens nucleus; Rh= rhomboid nucleus. The ATN, MT, and LT aggregates were based on neuroanatomical considerations per Mitchell and Dalrymple-Alford (2006).

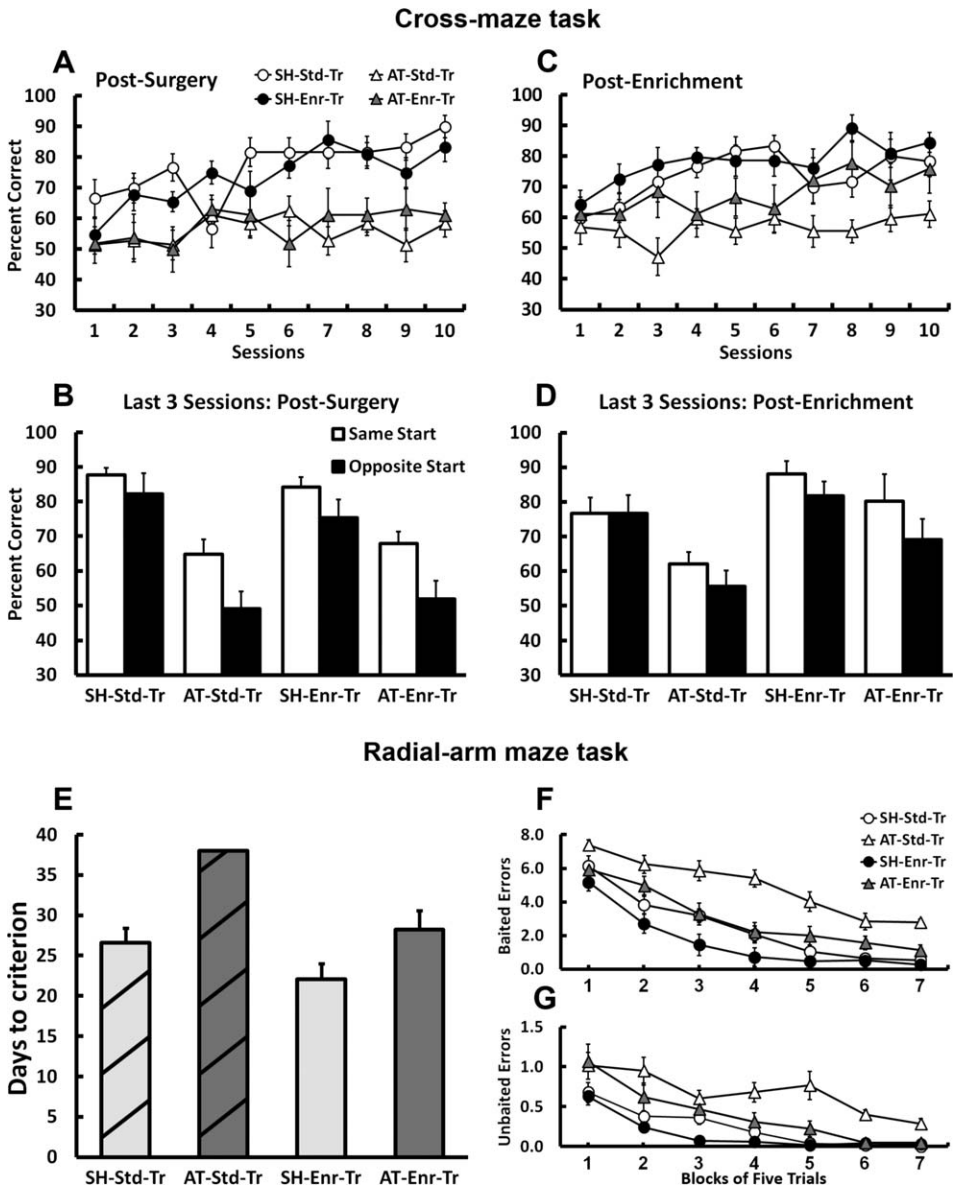

FIGURE 2. Spatial working memory in the cross-maze and radial-arm maze for the four trained groups. A) Mean (± SEM) performance across 10 sessions of postsurgery cross-maze testing. B) Postsurgery cross maze performance for the last three sessions expressed separately for the "same start position" and "opposite start position" trials. C) Same as (A), but showing 10 sessions of postenrichment cross maze testing. D) Same as (B), but showing different trials types over last three sessions of postenrichment cross maze testing. E) Mean number of days taken to reach criterion in the radial-arm maze task. F) Mean number of re-visits to baited arms shown over blocks of seven trials. G) Mean number of re-visits to the un-baited arm shown over blocks of seven trials.

criterion there were highly significant effects for Lesion ($F_{(1,41)} = 25.44$, $P < 0.001$; $d = 1.46$, CI 0.86–2.05) and Housing ($F_{(1,41)} = 16.90$, $P < 0.001$; $d = 1.15$, CI 0.55–1.74), but no interaction ($F_{(1,41} = 2.28$, ns). Post hoc Newman-Keuls tests confirmed that the AT-Std-Tr group was severely impaired on this measure compared with all other groups ($P < 0.001$). This deficit was ameliorated in the AT-Enr-Tr group, which did not differ from the SH-Std group ($P > 0.50$). The SH-Enr-Tr group reached criterion more quickly on average than the SH-Std-Tr group ($P < 0.08$) although not significantly, but more rapidly than the AT-Enr-Tr group ($P < 0.05$).

In keeping with the data for days to criterion, ATN lesions produced a clear deficit in terms of revisits (errors) to baited arms only (Lesion Effect, $F_{(1,41)} = 49.94$, $P < 0.001$; $d = 1.86$, CI 1.26–2.46). This measure produced both a Housing main effect ($F_{(1,41)} = 26.52$, $P < 0.001$; $d = 1.25$, CI 0.65–1.84) and a near-significant Lesion × Housing interaction ($F_{(1,41)} = 3.70$, $P = 0.07$; Fig. 2F). All groups exhibited a reduction in baited revisits over time (Blocks Effect,

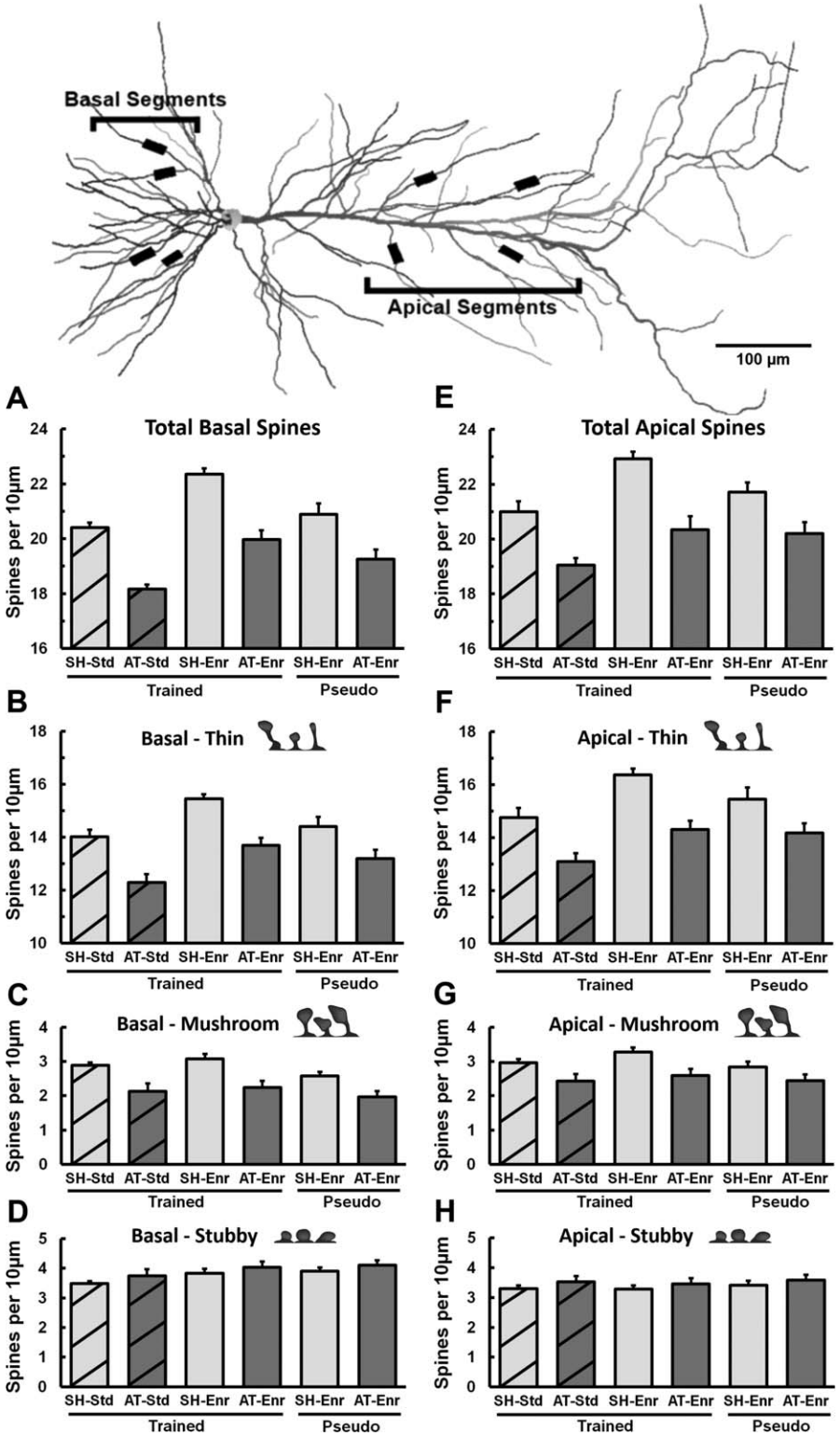

FIGURE 3. Basal and apical CA1 spine density per 10 µm shown for total (combined) spines as well as thin, mushroom and stubby spines (examples of spine types are shown next to graph headings). The four groups on the left in each graph were all trained and used to compare Lesion by Housing. The four groups on the right in each graph were all enriched and were used to compare Training by Pseudo-training. Top panel) Model of a CA1 neuron showing example locations of the 20 µm to 25 µm basal and apical segments taken for spine density analysis. A) Total basal spine density. B) Basal thin spine density. C) Basal mushroom spine density. D) Basal stubby spine density. E) Total apical spine density. F) Apical thin spine density. G) Apical mushroom spine density. H) Apical stubby spine density.

$F_{(6,246)} = 105.62$, $P < 0.001$), which was less rapid in AT rats (Lesion × Blocks, $F_{(6,246)} = 2.31$, $P < 0.05$), and more rapid in enriched rats (Housing × Blocks, $F_{(6,246)} = 2.86$, $P < 0.02$). Post hoc Newman-Keuls tests on the overall mean errors showed that the performance of the AT-Enr-Tr group did not differ from that of the SH-Std-Tr group ($P > 0.15$). The SH-Enr-Tr group had fewer baited revisits than all other groups ($P < 0.05$), whereas AT-Std-Tr had substantially more revisits than all other groups ($P < 0.001$).

Revisits to the single unbaited arm produced a similar pattern of results (Fig. 2G). The ATN lesion groups showed an increased number of unbaited errors ($F_{(1,41)} = 54.78$, $P < 0.001$; $d = 2.05$, CI 1.45–2.65) and enriched groups exhibited reduced unbaited errors ($F_{(1,41)} = 15.30$, $P < 0.001$; $d = 0.96$, CI 0.38–1.57). In this instance, there was a significant Lesion × Housing interaction ($F_{(1,41)} = 4.36$, $P < 0.05$). There was a highly significant effect of Blocks ($F_{(6,246)} = 30.48$, $P < 0.001$), but no interactions between Blocks and any other factor ($F < 1.8$). The two sham groups did not differ in terms of the number of unbaited errors ($P > 0.20$), whereas all other group comparisons differed significantly ($P < 0.02$).

CA1 Spine Density: ATN Lesion and Enrichment Effects in Trained Rats

Mean CA1 spine density in each group and example locations of selected dendritic segments used are shown in Figure 3. Examples of basal dendritic segments used for spine analysis are shown in Figure 4. Confirming our primary hypothesis, total spine density was markedly reduced by ATN lesions in rats housed in standard conditions. This effect of ATN lesions was reversed by enrichment, returning to a similar density to that observed in sham standard-housed rats ($P > 0.15$) albeit lower than that found in the SH-Enr-Tr group ($P < 0.001$; compare the four groups to the left of each graph in Fig. 3). The two way ANOVA of total basal spine density per 10 μm confirmed extremely large main effects of both Lesion ($F_{(1,41)} = 104.50$, $P < 0.001$; $d = 2.17$, CI 1.57–2.77) and Housing ($F_{(1,41)} = 69.37$, $P < 0.001$; $d = 1.63$, CI 1.03–2.23), but no interaction (Lesion × Housing, $F < 1.5$). With respect to two key comparisons, the effect size for ATN lesions in the AT-Std-Tr versus SH-Std-Tr rats was $d = 3.77$, CI 2.89–4.65, and the effect size for enrichment in the AT-Std-Tr versus AT-Enr-Tr rats was $d = 2.27$, CI 1.36–3.18. Analysis restricted to the thin basal spines (68.5% of total basal spines) produced a similar pattern of results (Lesion, $F_{(1,41)} = 46.39$, $P < 0.001$; Housing, $F_{(1,41)} = 30.77$, $P < 0.001$; Lesion × Housing, $F < 1.0$). While the analysis of basal mushroom spines (12.5% of total basal spines) again produced a Lesion effect ($F_{(1,41)} = 20.81$, $P < 0.001$), there was no Housing effect ($F < 1.0$; Lesion × Housing, $F < 1.0$). There were no main effects or interaction associated with basal stubby spine density ($F < 2.5$; 19% of total basal spines).

Analysis of variance of the total apical spine density per 10μm also revealed highly significant main effects of Lesion ($F_{(1,41)} = 43.87$, $P < 0.001$; $d = 1.83$, CI 1.23–2.43) and Housing ($F_{(1,41)} = 22.68$, $P < 0.001$; $d = 1.25$, CI 0.65–1.84), but no Lesion × Housing interaction ($F < 1.0$). As with total spines, the density of thin apical spines (70.5% of total apical spines) was also associated with Lesion ($F_{(1,41)} = 36.55$, $P < 0.001$) and Housing ($F_{(1,41)} = 21.12$, $P < 0.001$) effects, but no Lesion × Housing interaction ($F < 1.0$). Analysis of apical mushroom spines (13.5% of total apical spines) produced a Lesion effect ($F_{(1,41)} = 14.13$, $P < 0.001$) but no Housing effects ($F < 2.0$; Lesion × Housing interaction, $F < 1.0$). Apical stubby spine density (16% of total apical spines) was not associated with any main effects or interaction ($F < 1.5$).

CA1 spine density: Training Effects in Enriched Groups

Rats that received explicit spatial memory training and enrichment showed more total basal, but not apical, spines than those given pseudo-training procedures and enrichment (compare the 4 enriched groups to the right of each graph in Fig. 3). The ANOVA of total basal spine density per 10 μm across the trained and pseudo-trained enriched groups produced a main effect of Lesion ($F_{(1,36)} = 41.16$, $P < 0.001$; $d = 1.92$, CI 1.28–2.56), and Training ($F_{(1,36)} = 12.14$, $P < 0.002$; $d = 0.92$, CI 0.28–1.56), but no indication that the Training effect varied across the two surgery conditions (Lesion × Training, $F < 1.5$). The analysis for basal thin spines also produced a Lesion effect ($F_{(1,36)} = 28.40$, $P < 0.001$) and a Training effect ($F_{(1,36)} = 7.87$, $P < 0.01$), but no interaction ($F < 1.0$) and the same was found for basal mushroom spines (Lesion effect, $F_{(1,36)} = 20.09$, $P < 0.001$; Training effect, $F_{(1,36)} = 5.57$, $P < 0.05$). No differences across these groups were found for basal stubby spine density ($F < 1.0$).

Analysis of variance of total apical spine density per 10μm across the four enriched groups produced a Lesion effect ($F_{(1,36)} = 29.75$, $P < 0.001$; $d = 1.78$, CI 1.14–2.42), but the Training effect did not reach significance for this measure ($F_{(1,36)} = 3.28$, $P < 0.08$; $d = 0.58$, CI −0.062–1.22; Lesion × Training, $F < 1.0$). Analysis of the apical thin spines also produced a Lesion effect ($F_{(1,36)} = 24.73$, $P < 0.001$), but again no effect of Training ($F < 2.5$; Lesion × Training interaction, $F < 1.5$). Mushroom spines were associated with a clear Lesion effect ($F_{(1,36)} = 11.08$, $P < 0.005$) and a Training effect that neared significance ($F_{(1,36)} = 3.13$, $P < 0.09$; Lesion × Training, $F < 1.0$). The analysis of apical stubby spines produced no main effects or interaction ($F < 1.0$).

Rgb Fusiform Apical Spine Density: ATN Lesion and Enrichment Effects in Trained Rats

Example locations of selected dendritic segments used are shown in Figure 5A. Mean Rgb spine density in each group is shown in Figure 5B and examples of the relative difference in apical spine density between SH and AT rats is shown in Figure 5C. Total spine density in the superficial layer of the Rgb was also was markedly reduced by ATN lesions, but there was

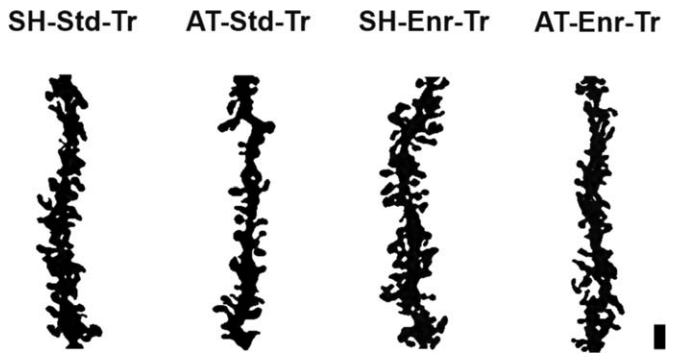

FIGURE 4. Photomicrographs (×63 glycerol objective, NA 1.3, with ×2 digital zoom) of representative Golgi-stained basal dendritic segments from the four main experimental groups. Individual serial optical sections were overlaid to generate the two-dimensional projection images of the segments presented here (background removed). Spine counts were conducted using Neurolucida software to process the original image stacks. The spine density per 10 μm for these segments was: SH-Std-Tr = 20.32; AT-Std-Tr = 18.00; SH-Enr-Tr = 22.32; AT-Enr-Tr = 20.14. Scale bar = 2 μm.

no effect of enrichment. ANOVA of total apical spine density per 10μm across the four Lesion by Housing groups confirmed a Lesion main effect ($F_{(1,41)} = 36.13$, $P < 0.0001$; $d = 1.88$, CI 1.28–2.48) but no Housing effect or Lesion × Housing interaction ($F < 1.0$). This lesion-induced reduction represented a reduction in thin apical spines ($F_{(1,41)} = 31.19$, $P < 0.0001$; Housing and Lesion × Housing, $F < 2.0$) as there were no effects restricted to either mushroom or stubby spines (main effects and interactions, $F < 2.0$). In these Rgb neurons thin spines constituted 76% of total apical spines, mushroom spines made up only 6% of total spines, and stubby spines accounted for 18% of total spines.

Rgb Fusiform Apical Spine Density: Training Effects in Enriched Groups

Analysis of variance of the four enriched Lesion by Training groups produced a Lesion main effect ($F_{(1,41)} = 20.67$, $P < 0.0001$; $d = 1.52$, CI 0.88–2.16) but there was no evidence of a Training effect or Training × Housing interaction ($F < 1.0$). The Lesion effect was evident for thin apical spines only ($F_{(1,41)} = 19.50$, $P < 0.0001$; Housing and Lesion × Housing, $F < 1.0$) with no main effects or interactions associated with mushroom or stubby spines ($F < 1.0$).

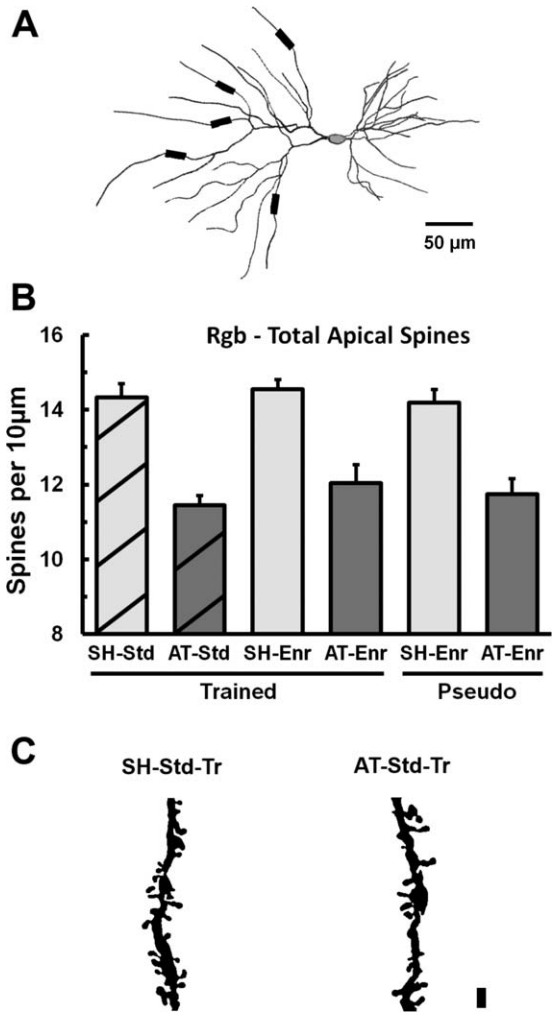

FIGURE 5. Spine density of apical dendritic segments from fusiform layer II/III pyramidal neurons from the retrosplenial granular b cortex (Rgb). A) Model of a fusiform pyramidal Rgb neuron showing example locations in layer I for the 20 μm to 25 μm apical segments taken for spine density analysis. B) Total apical spine density per 10 μm. The four groups on the left in each graph were all trained and used to compare Lesion by Housing. The four groups on the right in each graph were all enriched and were used to compare Training by Pseudo-training. C) Individual serial optical sections (100x oil objective, NA 1.3) were overlaid to generate these two-dimensional projection images of representative segments from SH-Std-Tr and AT-Std-Tr rats. The spine density from the original image stacks for these segments was: SH-Std-Tr = 14.69; AT-Std-Tr = 11.85. Scale bar = 2 μm.

Regression Analysis

Stepwise regression was used to first determine the extent to which spine density in the different areas made contributions to spatial memory. CA1 basal spine density, CA1 apical spine density, and Rgb apical spine density were submitted to stepwise regression, with baited arm errors in the radial-arm maze as the dependent variable. Their initial simple correlations were −0.77, −0.66, and −0.65, respectively ($N = 45$, $P < 0.001$). As a result CA1 basal spine density was the variable included at the first step ($F_{change}(1,43) = 62.25$, $P < 0.001$) and Rgb apical spine density added significantly at the second step ($F_{change}(1,42) = 5.18$, $P = 0.03$). CA1 apical did not enter the equation as it was highly correlated with CA1 basal ($r = 0.89$). When CA1 apical was forced into the equation the distribution of variance was: CA1 basal unique = 9.6%; Rgb apical unique- = 4.5%; CA1 apical unique = 0.3%; share*d* = 49.5% accounting for a total of 64.0% of the variance in baited arm errors. Thus the bulk of the simple correlations are accounted for by the shared variance, although both Rgb apical and especially

CA1 basal have minor additional unique explanatory power over and above the variance they share between them.

To test how far these correlational results were the product of treatment effects, we added Lesion, Housing and their interaction to the predictors. The stepwise regression found significant effects of CA1 basal spines and Rgb apical spines, as before, with the Lesion × Housing interaction providing additional explanatory power. The additional predictive power of Lesion × Housing was unique and it did not share any of the explanatory power of the spine variables. This suggests that the interaction term is not the cause of the observed relationship between spines and behaviour. However, there were no significant effects when we carried out the original spine analysis separately for each treatment group although the largest correlations were found in the lesion groups (with a maximum value of −0.51). When we forced CA1 basal spines (the most powerful original predictor) into an equation with Lesion, Housing and their interaction this spine measure had virtually no unique variance (0.4%) while Lesion and Housing factors retained about 5% leaving shared variance of 54% within a total explained variance of 72%. Thus Lesion and Housing affect both behaviour and spine density; but the changes in spine density are better predictors of behaviour (since they are extracted preferentially with Lesion and Housing failing to enter the equation). Spine density, therefore, appears to mediate an important part of the Lesion and Housing effects on behaviour. Equally, Lesion and Housing have small amounts of additional unique variance, which could be due, for example, to changes in spine density in regions that we did not assess.

DISCUSSION

The current study showed that ATN lesions in standard-housed rats substantially reduce dendritic spine density in the hippocampal CA1 area and the Rgb–confirming our main hypothesis that ATN injury reduces microstructure integrity in these brain regions. In the hippocampus these excitatory synaptic markers were reduced for both thin spine density and mushroom spine density in basal CA1 dendritic segments from tertiary or quarternary branches in the stratum oriens and lateral oblique apical CA1 dendrites emerging from a primary apical trunk in the stratum radiatum. ATN lesions also reduced apical spine density in Rgb fusiform layer II/III neurons with respect to thin spines. Validation of the potential behavioural significance of these findings was evident from impaired spatial memory in standard-housed rats with ATN lesions.

As we have shown previously, subsequent exposure to an enriched environment reversed the substantial spatial working memory deficits in the cross-maze produced by ATN lesions (Loukavenko et al., 2007). Evidence of enrichment-induced recovery in rats with ATN lesions was extended here to the radial-arm maze task, where substantially more working memory errors and failure to reach criterion were found in standard-housed rats with ATN lesions compared with other groups. A more novel result was that the lesion-induced deficits in CA1 thin, but not mushroom, spines were reversed by exposure to enrichment. Enrichment did not affect Rgb spines in either ATN-lesioned or sham rats. Furthermore, enriched rats that experienced spatial memory training had increased CA1 basal spine density, but not Rgb spine density, when compared with pseudo-trained enriched rats given comparable task-related experience. This finding suggests that some aspects of hippocampal spine density in particular were relevant to spatial learning and memory beyond general behavioural testing.

This study provides the first report of microstructural changes in the hippocampus after ATN lesions. Our results strongly support the specific idea (Vann, 2010; Aggleton et al., 2010) that the ATN have a potent influence on the hippocampus rather than simply acting as a relay between the hippocampus and prefrontal cortex. Dendritic spine density and morphology are linked to the processing of cognition-related synaptic information (Jedlicka et al., 2008; González-Ramírez et al., 2014). Increases or decreases in dendritic surface reflect changes in synaptic organisation and reduced CA1 spine density suggests a loss of excitatory input to these hippocampal neurons (Kolb et al., 2003; Bourne and Harris, 2007). The AT-Std-Tr group exhibited a mean reduction of ∼10% in both basal and apical CA1 hippocampal spine density compared with the SH-Std-Tr group. To put this change into context, the effect on CA1 basal spine density was if anything larger than the behavioural effects of ATN lesions in standard-housed rats (effect size, $d = 3.77$, 95% CI 2.89–4.65, for basal spines; $d = 2.40$, CI 1.80–3.00, for spatial working memory before introducing enrichment). This effect size for the basal spines means that there was virtually no overlap (∼6%) in the distribution of the counts in the standard-housed intact rats compared with the distribution of counts in those with ATN lesions. Other reports also suggest that the hippocampus may not be fully functional after ATN injury, but the effect size is weaker for pCREB ($d = 0.81$ to $d = 1.32$) and IEG markers ($d = 0.41$ to $d = 1.05$; Jenkins et al., 2002a,b; Dumont et al., 2012; Dupire et al., 2013). The lower CA1 spine density associated with ATN lesions in the current study may represent a significant reduction in experience-dependent plasticity in a sub-region thought to add temporal context to events (Rolls and Kesner, 2006; Langston et al., 2010) and which may affect the plasticity and function of place fields generated by these CA1 neurons.

The neural connections between the ATN and extended hippocampal system may explain the changes to CA1 after ATN lesions. The ATN can exert an effect on the hippocampus primarily through two routes, its direct projections to the parahippocampal region and its indirect projections via the retrosplenial cortex (Wyss and Van Groen, 1992; Shibata 1993). Specifically, the ATN have widely distributed direct connections to the presubiculum, parasubiculum, subiculum, and medial entorhinal cortex (Shibata, 1993; Aggleton et al., 2010). The retrosplenial cortex also has afferent connections with the presubiculum, parasubiculum, and medial entorhinal

cortex (Wyss and Van Groen, 1992). The presubiculum, parasubiculum, and subiculum influence the CA1 through their projections to the entorhinal cortex, especially layer III of the medial entorhinal cortex and its direct connections to CA1, as well as through their projections to the dentate gyrus (Witter et al., 2014). The subiculum is primarily an output structure of the hippocampus, but it also has feedback projections to CA1 via the presubiculum and medial entorhinal cortex. Recent neuroanatomical description of the parahippocampal-hippocampal network (Witter et al., 2014) suggests that the influence of ATN lesions on CA1 morphology may primarily be through indirect influence on the entorhinal cortex by way of changes to the hippocampal input structures of the presubiculum and parasubiculum.

The retrosplenial cortex has been a locus of much more marked and consistent IEG changes after ATN lesions than the hippocampus, perhaps because of its direct connections with the ATN (Jenkins et al., 2004; Poirier and Aggleton, 2009; Dupire et al., 2013). The retrosplenial cortex also shows reductions in pCREB and cytochrome oxidase after ATN lesions (Dumont et al., 2012; Dupire et al., 2013; Mendez-Lopez et al., 2013). Arguably the most convincing example of this retrosplenial deactivation is that following unilateral ATN lesions it was possible to induce long-term depression in a slice of retrosplenial cortex in the unaffected hemisphere, but not in a slice ipsilateral to the lesion (Garden et al., 2009). The current study complements these findings by showing a decrease in excitatory synaptic function in the form of a mean reduction of about 20% (effect size, $d = 1.88$) in layer I apical spine density in fusiform pyramidal neurons that have their cell bodies located in layers II/III. These superficial layers of the Rgb show the most marked IEG changes ($d = 1.98$–4.60). Although spine changes in the Rgb layer with dense afferent connections from the ATN may not be surprising, this finding has not been shown previously.

ATN lesions produced clear spatial working memory deficits in the cross-maze after surgery, which as expected persisted in rats that remained in standard cages. The standard-housed AT rats showed relatively good performance when sample and test runs were from the same start position, especially after extended behavioral training. In contrast, they performed poorly when sample and test runs were from different start positions. A simple olfaction-based strategy would not explain these performance differences across the two types of trial. It is likely that the poorer performance on the different start position trials reflected more reliance on the use of allocentric or directional cues in these trials, as suggested in other reports using T-maze or cross maze alternation (Aggleton et al., 1996; Warburton et al., 2001; Loukavenko et al., 2007).

The radial-arm maze is another spatial memory test in which standard-housed rats with ATN lesions commonly make substantial errors (Aggleton et al., 1996; Mair et al., 2003; Moran and Dalrymple-Alford, 2003; Mitchell and Dalrymple-Alford, 2006; Sziklas and Petrides, 2007). The use of one unbaited arm here resulted in none of the 12 AT-Std-Tr rats being able to reach criterion in 35 days of testing. By contrast, enrichment after ATN lesions resulted in two out of nine rats being unable to reach criterion. Enrichment also returned the average number of radial-arm maze errors to a level comparable to that of the SH-Std-Tr group. The apparent contradiction between improved radial-arm maze performance found here and the failure to find recovery in the radial-arm maze in enriched AT rats in a previous study (Loukavenko et al., 2007) can be accounted by procedural differences. That study looked at discrimination between different pairs of arms and rotated the maze while the rats remained in the central hub, producing additional distraction and vestibular stimulation which is known to impair spatial discrimination (Kirwan et al., 2005). Regression analysis showed that radial-arm maze performance was best predicted by CA1 basal spine density. However, this association was in turn driven mostly by the spine density changes produced by ATN lesions and enrichment.

The hippocampal CA1 region has been linked with plasticity and recovery of function after brain injury (Bendel et al., 2005; Neves et al., 2008). In the current study, the AT-Enr-Tr group showed large effects when compared with the AT-Std-Tr group, with a mean increase of 9.0% in basal and 6.4% in apical CA1 spine density; indeed, spine density in the AT-Enr-Tr group was comparable to that of the SH-Std-Tr group. The percentage increase for basal spines in our enriched sham rats (8.6%) was similar to that of other studies of enrichment in intact rats (Moser et al., 1994, 1997) and marmosets (Kozorovitskiy et al., 2005). We do not know the molecular mechanisms responsible for improved spine density after enrichment in rats with ATN lesions. Increased CREB function has been associated with recovery of CA1 spines and improved spatial memory in Alzheimer's type transgenic mice (Yiu et al., 2011), so CREB function could be one mechanism for the changes we observed. However, neither pCREB nor c-Fos expression have been increased in the hippocampus by enrichment in AT rats (Dupire et al., 2013). An alternative mechanism may be an increase in brain-derived neurotrophic factor (BDNF), which is elevated in intact enriched rats (Ickes et al., 2000) and in ischemic rats after enrichment (Puurunen et al., 2001). Components of the BDNF signalling cascade, such as histone 3 and mitogen- and stress-activated kinase 1**,** have also been linked with the beneficial effects of environmental enrichment (Fischer et al., 2007; Corrêa et al., 2012). A relative increase in CA1 spines has also been found after enrichment of rats with subicular lesions, but in this case there was no increase in BDNF levels in enriched rats (Bindu et al., 2007). Additional study is therefore needed to examine whether BDNF and its metabolic pathways provide the mechanisms of recovery of CA1 spine density and behavioural function after ATN lesions.

Increased dendritic spines in CA1 have been associated with spatial memory through comparisons of trained with untrained rats or rats that were trained in an enriched spatial environment relative to non-trained single-housed or pair-housed rats (Moser et al., 1994, 1997; Marrone, 2007; González-Ramírez et al., 2014). Incidental experience with training procedures, such as food reward, sensorimotor requirements or training-associated stress may also have an influence on spine

morphology. Previous studies on CA1 spine number that included explicit pseudo-trained controls to account for some of these incidental factors employed simple olfactory discrimination tasks, which do not depend on CA1 integrity for normal performance (Knafo et al., 2004; Restivo et al., 2006; Kesner, 2013). In the current study, enriched rats trained on tasks that are highly sensitive to hippocampal lesions showed more CA1 basal spines than enriched rats that were given a comparable pseudo-training procedure. This evidence complements previous findings that spatial training exerts an effect through these basal spines (Moser et al., 1994, 1997; González-Ramírez et al., 2014) by providing novel support that, at least in enriched trained rats, increases in CA1 spine density are specifically related to improved spatial working memory beyond non-specific task-related factors.

The alterations in synaptic plasticity evident from the reduced spine density after ATN lesions are likely to impact CA1 cell function and thus temporal encoding and place learning (Kesner, 2013). The specific effects of reductions in thin and mushroom spine density are less clear. Thin spines are generally regarded as transient but structurally flexible enabling them to enlarge and stabilize or shrink and dismantle depending on whether they are required to accommodate new, enhanced, or recently weakened inputs associated with learning (Kasai et al., 2003; Bourne and Harris, 2007). Mushroom spines are regarded as more stable and may represent a more permanent physical substrate that contributes to longer-term memory (Kasai et al., 2003; Bourne and Harris, 2007). Hence it is possible that the substantial loss of thin CA1 spines as a consequence of ATN lesions may contribute to impairments in new learning, while the loss of mushroom CA1 spines may reflect weaker substrates for previously acquired mnemonic information. In the current study enrichment was associated with an increase in thin spines only, which implies that enrichment will have a greater impact on new learning and that any longer-term memory traces that depend on the CA1 region may be less influenced by enrichment. Thin spine plasticity has a key role in the induction of long term potentiation (LTP) (Matsuzaki et al., 2004) and altered network dynamics in CA1 due to enrichment may augment information processing in the hippocampus and enhance hippocampal-dependent learning and memory (Irvine and Abraham, 2005; Artola et al., 2006; Eckert et al., 2010). Thus the recovery of thin spines through enrichment may normalize the capacity for LTP induction and thus memory capability. The recovery of thin, but not mushroom spines, was an unexpected finding. Given that a selective loss of thin spine plasticity is associated with impaired spatial memory in aged rats (González-Ramírez et al., 2014), a selective pattern of recovery of thin spines is consistent with the ability of enrichment to improve spatial memory after ATN lesions. In enriched rats, the effect of training as opposed to pseudo-training also produced a substantial increase in thin spines and a far weaker effect was also evident for mushroom spines. Nonetheless, a failure to increase mushroom spines suggests a neural substrate that may limit the degree of behavioural recovery associated with enrichment.

The current study was by necessity restricted to two subregions, albeit in structures highly relevant to the ATN. Aside from different brain regions, other hippocampal or retrosplenial subregions may also show changes after ATN lesions that are associated with recovery induced by enrichment, which limits the generality of our findings. ATN lesions induced changes in both CA1 spine density and apical spines from Rgb fusiform layer II/III neurons, yet recovery with enrichment was evident for the former measure only. This difference implies that either enrichment produces a selective and partial recovery or that the changes to the superficial retrosplenial cortex are not always essential for the behavioural impairments associated with ATN lesions. It is also possible, however, that recovery of spine number in the superficial region of this restroplenial cortex is task-dependent. For example, standard spatial memory tasks are often only mildly affected by lesions to the retrosplenial cortex, whereas spatial tasks that place internal and external maze cues in conflict produce a more robust deficit (Pothuizen et al., 2010). Thus recovery of spine number in the retrosplenial cortex may have been observed if we had used this alternate spatial task. Another possibility is that enrichment effects in the Rgb depend on other mechanisms than dendritic morphology. Enrichment does not, however, change the severely reduced c-Fos expression in the retroplenial cortex after ATN lesions (Dupire et al. 2013). On balance, the current study suggests that changes to the hippocampus are especially relevant to both deficits and recovery after ATN lesions.

In summary, these findings provide evidence of an influence of ATN lesions on both the hippocampus and retrosplenial cortex, at the level of spine morphology. Thus our results provide new support for a strong influence of the ATN on the extended hippocampal system (Aggleton and Brown, 2006; Aggleton et al., 2010). Postoperative enrichment in rats with ATN lesions resulted in recovery of spine density in the hippocampal CA1, but not in the Rgb, accompanied by improvements in memory performance. Further research is needed to determine whether ATN lesions induce irreversible changes in the retrosplenial cortex or whether recovery in this brain region can be found in measures other than dendritic morphology. Hippocampal CA1 spines are associated with spatial memory training at least with the tasks used here; while Rgb spines appear less so. Other treatments should be examined to determine whether they can recover CA1 or Rgb spines after ATN lesions, as well as other deficits produced by ATN lesions, and their association with improved recovery of function.

REFERENCES

Aggleton JP. 2008. Understanding anterograde amnesia: Disconnections and hidden lesions. Q J Exp Psychol 61:1441–1471.

Aggleton JP. 2012. Multiple anatomical systems embedded within the primate medial temporal lobe: Implications for hippocampal function. Neurosci Biobehav Rev 36:1579–1596.

Aggleton JP, Brown MW. 1999. Episodic memory, amnesia, and the hippocampal-anterior thalamic axis. Behav Brain Sci 22: 425–489.

Aggleton JP, Brown MW. 2006. Interleaving brain systems for episodic and recognition memory. Trends Cogn Sci 10:455–463.

Aggleton JP, Hunt PR, Nagle S, Neave N. 1996. The effects of selective lesions within the anterior thalamic nuclei on spatial memory in the rat. Behav Brain Res 81:189–198.

Aggleton JP, O'Mara SM, Vann SD, Wright NF, Tsanov M, Erichsen JT. 2010. Hippocampal-anterior thalamic pathways for memory: Uncovering a network of direct and indirect actions. Eur J Neurosci 31:2292–2307.

Artola A, von Frijtag JC, Fermont PC, Gispen WH, Schrama LH, Kamal A, Spruijt BM. 2006. Long-lasting modulation of the induction of LTD and LTP in rat hippocampal CA1 by behavioural stress and environmental enrichment. Eur J Neurosci 23:261–272.

Bendel O, Bueters T, von Euler M, Ove Ögren S, Sandin J, von Euler G. 2005. Reappearance of hippocampal CA1 neurons after ischemia is associated with recovery of learning and memory. J Cereb Blood Flow Metab 25:1586–1595.

Bindu B, Alladi PA, Mansooralikhan BM, Srikumar BN, Raju TR, Kutty BM. 2007. Short-term exposure to an enriched environment enhances dendritic branching but not brain-derived neurotrophic factor expression in the hippocampus of rats with ventral subicular lesions. Neuroscience 144:412–423.

Bourne JN, Harris KM. 2007. Do thin spines learn to be mushroom spines that remember? Curr Opin Neurobiol 17:381–386.

Carlesimo GA, Lombardi MG, Caltagirone C. 2011. Vascular thalamic amnesia: A reappraisal. Neuropsychologia 49:777–789.

Cenquizca LA, Swanson LW. 2006. An analysis of direct hippocampal cortical field CA1 axonal projections to the diencephalon in rats. J Comp Neurol 497:101–114.

Corrêa SA, Hunter CJ, Palygin O, Wauters SC, Martin KJ, McKenzie C, McKelvey K, Morris RG, Pankratov Y, Arthur JS, Frenguelli BG. 2012. MSK1 regulates homeostatic and experience-dependent synaptic plasticity. J Neurosci 32:13039–13051.

De Simoni A, Griesinger CB, Edwards FA. 2003. Development of rat CA1 neurones in acute versus organotypic slices: Role of experience in synaptic morphology and activity. J Physiol 550:135–147.

Dumont JR, Aggleton JP. 2013. Dissociation of recognition and recency memory judgements after anterior thalamic nuclei lesions in rats. Behav Neurosci 127:415–431.

Dumont JR, Amin E, Poirier GL, Albasser MM, Aggleton JP. 2012. Anterior thalamic lesions in rats disrupt markers of neural plasticity in distal limbic brain regions. Neuroscience 224:81–101.

Dupire A, Kant P, Mons N, Marchand A, Dalrymple-Alford J, Wolff M. 2013. A role for anterior thalamic nuclei in affective cognition: Interaction with environmental conditions. Hippocampus 23:392–404.

Eckert MJ, Bilkey DK, Abraham WC. 2010. Altered plasticity in hippocampal CA1, but not dentate gyrus, following long-term environmental enrichment. J Neurophysiol 103:3320–3329.

Fellow BJ. 1967. Change stimulus sequences for discrimination tasks. Psychol Bull 67:87–92.

Fischer A, Sananbenesi F, Wang X, Dobbin M, Tsai LH. 2007. Recovery of learning and memory is associated with chromatin remodelling. Nature 447:178–182.

Garden DL, Massey PV, Caruana DA, Johnson B, Warburton EC, Aggleton JP, Bashir ZI. 2009. Anterior thalamic lesions stop synaptic plasticity in retrosplenial cortex slices: Expanding the pathology of diencephalic amnesia. Brain 132:1847–1857.

González-Ramírez MM, Velázquez-Zamora DA, Olvera-Cortés ME, González-Burgos I. 2014. Changes in the plastic properties of hippocampal dendritic spines underlie the attenuation of place learning in healthy aged rats. Neurobiol Learn Mem 109:94–103.

Harding A, Halliday G, Caine D, Kril J. 2000. Degeneration of anterior thalamic nuclei differentiates alcoholics with amnesia. Brain 123:141–154.

Harris KM, Jensen FE, Tsao B. 1992. Three-dimensional structure of dendritic spines and synapses in rat hippocampus (CA1) at postnatal day 15 and adult ages: Implications for the maturation of synaptic physiology and long-term potentiation. J Neurosci 12: 2685–2705.

Henry J, Petrides M, Laurent St M, Sziklas V. 2004. Spatial conditional associative learning: Effects of thalamo-hippocampal disconnection in rats. Neuroreport 15:1–5.

Ickes BR, Pham TM, Sanders LA, Albeck DS, Mohammed AH, Granholm AC. 2000. Long-term environmental enrichment leads to regional increases in neurotrophin levels in rat brain. Exp Neurol 164:45–52.

Irvine GI, Abraham WC. 2005. Enriched environment exposure alters the input-output dynamics of synaptic transmission in area CA1 of freely moving rats. Neurosci Lett 391:32–37.

Jedlicka P, Vlachos A, Schwarzacher SW, Deller T. 2008. A role for the spine apparatus in LTP and spatial learning. Behav Brain Res 192:12–19.

Jenkins TA, Dias R, Amin E, Aggleton JP. 2002a. Changes in Fos expression in the rat brain after unilateral lesions of the anterior thalamic nuclei. Eur J Neurosci 16:1425–1432.

Jenkins TA, Dias R, Amin E, Brown MW, Aggleton JP. 2002b. Fos imaging reveals that lesions of the anterior thalamic nuclei produce widespread limbic hypoactivity in rats. J Neurosci 22:5230–5238.

Jenkins TA, Vann SD, Amin E, Aggleton JP. 2004. Anterior thalamic lesions stop immediate early gene activation in selective laminae of the retrosplenial cortex: Evidence of covert pathology in rats? Eur J Neurosci 19:3291–3304.

Kasai H, Matsuzaki M, Noguchi J, Yasumatsu N, Nakahara H. 2003. Structure-stability-function relationships of dendritic spines. Trends Neurosci 26:360–368.

Kesner RP. 2013. Role of the hippocampus in mediating interference as measured by pattern separation processes. Behav Process 93: 148–154.

Kirwan CB, Gilbert PE, Kesner RP. 2005. The role of the hippocampus in the retrieval of a spatial location. Neurobiol Learn Mem 83: 65–71.

Kolb B, Gibb R, Robinson TE. 2003. Brain plasticity and behavior. Curr Dir Psychol 14:1–5.

Kozorovitskiy Y, Gross CG, Kopil C, Battaglia L, McBreen M, Stranahan AM, Gould E. 2005. Experience induces structural and biochemical changes in the adult primate brain. Proc Natl Acad Sci USA 102:17478–17482.

Knafo S, Ariav G, Barkai E, Libersat F. 2004. Olfactory learning-induced increase in spine density along the apical dendrites of CA1 hippocampal neurons. Hippocampus 14:819–825.

Langston RF, Stevenson CH, Wilson CL, Saunders I, Wood ER. 2010. The role of the hippocampal subregions in memory for stimulus associations. Behav Brain Res 215:275–291.

Loukavenko E, Ottley M, Moran J, Wolff M, Dalrymple-Alford J. 2007. Towards therapy to relieve memory impairment after anterior thalamic lesions: Improved spatial working memory after immediate and delayed post-operative enrichment. Eur J Neurosci 26:3267–3276.

Mair RG, Burk JA, Porter MC. 2003. Impairment of radial maze delayed nonmatching after lesions of anterior thalamus and parahippocampal cortex. Behav Neurosci 117:596–605.

Marrone DF. 2007. Ultrastructural plasticity associated with hippocampal dependent learning: A meta-analysis. Neurobiol Learn Mem 87:361–371.

Matsuzaki M, Honkura N, Ellis-Davies GR, Kasai H. 2004. Structural basis of long-term potentiation in single dendritic spines. Nature 429:761–766.

Mendez-Lopez M, Arias JL, Bontempi B, Wolff M. 2013. Reduced cytochrome oxidase activity in the retrosplenial cortex after lesions to the anterior thalamic nuclei. Behav Brain Res 250:264–273.

Mitchell AS, Dalrymple-Alford JC. 2006. Lateral and anterior thalamic lesions impair independent memory systems. Learn Mem 13: 388–396.

Moran JP, Dalrymple-Alford JC. 2003. Perirhinal cortex and anterior thalamic lesions: Comparative effects on learning and memory. Behav Neurosci 117:1326–1341.

Moreau PH, Tsenkina Y, Lecourtier L, Lopez J, Cosquer B, Wolff M, Dalrymple-Alford JC, Cassel JC. 2012. Lesions of the anterior thalamic nuclei and intralaminar nuclei: Place and visual discrimination learning in the water maze. Brain Struct Funct 218:657–667.

Moser MB, Trommald M, Andersen P. 1994. An increase in dendritic spine density on hippocampal CA1 pyramidal cells following spatial learning in adult rats suggests the formation of new synapses. Proc Natl Acad Sci USA 91:12673–12675.

Moser MB, Trommald M, Egeland T, Andersen P. 1997. Spatial training in a complex environment and isolation alter the spine distribution differently in rat CA1 pyramidal cells. J Comp Neurol 380: 373–381.

Neves G, Cooke SF, Bliss TV. 2008. Synaptic plasticity, memory and the hippocampus: A neural network approach to causality. Nat Rev Neurosci 9:65–75.

Paxinos G, Watson C. 1998. The Rat Brain in Stereotaxic Coordinates, 4th ed. San Diego, CA: Academic Press.

Poirier GL, Aggleton JP. 2009. Post-surgical interval and lesion location within the limbic thalamus determine extent of retrosplenial cortex immediate-early gene hypoactivity. Neuroscience 160:452–469.

Pothuizen HH, Davies M, Aggleton JP, Vann SD. 2010. Effects of selective granular retrosplenial cortex lesions on spatial working memory in rats. Behav Brain Res 208:566–575.

Puurunen K, Jolkkonen J, Sirvio J, Haapalinna A, Sivenius J. 2001. Selegiline combined with enriched-environment housing attenuates spatial learning deficits following focal cerebral ischemia in rats. Exp Neurol 167:348–355.

Restivo L, Roman FS, Ammassari-Teule M, Marchetti E. 2006. Simultaneous olfactory discrimination elicits a strain-specific increase in dendritic spines in the hippocampus of inbred mice. Hippocampus 16:472–479.

Rolls ET, Kesner RP. 2006. A computational theory of hippocampal function, and empirical tests of the theory. Prog Neurobiol 79:1–48.

Shibata H. 1993. Direct projections from the anterior thalamic nuclei to the retrohippocampal region in the rat. J Comp Neurol 337: 431–445.

Sziklas V, Petrides M. 2007. Contribution of the anterior thalamic nuclei to conditional learning in rats. Hippocampus 17:456–461.

van der Werf YD, Witter MP, Groenewegen HJ. 2002. The intralaminar and midline nuclei of the thalamus. Anatomical and functional evidence for participation in processes of arousal and awareness. Brain Res Brain Res Rev 39:107–140.

Vann SD. 2010. Re-evaluating the role of the mammillary bodies in memory. Neuropsychologia 48:2316–2327.

Vann SD. 2013. Dismantling the papez circuit for memory in rats. eLife 2:e00736.

Vann SD, Albasser MM. 2009. Hippocampal, retrosplenial, and prefrontal hypoactivity in a model of diencephalic amnesia: Evidence towards an interdependent subcortical-cortical memory network. Hippocampus 19:1090–1102.

Warburton EC, Baird A, Morgan A, Muir JL, Aggleton JP. 2001. The conjoint importance of the hippocampus and anterior thalamic nuclei for allocentric spatial learning: Evidence from a disconnection study in the rat. J Neurosci 21:7323–7330.

Witter MP, Canto CB, Couey JJ, Koganezawa N, O'Reilly KC. 2014. Architecture of spatial circuits in the hippocampal region. Phil Trans R Soc B 369:20120515.

Wolff M, Gibb SJ, Dalrymple-Alford JC. 2006. Beyond spatial memory: The anterior thalamus and memory for the temporal order of a sequence of odour cues. J Neurosci 26:2907–2913.

Wolff M, Gibb SJ, Cassel JC, Dalrymple-Alford JC. 2008. The extended hippocampal-diencephalic memory system: Enriched housing promotes recovery of the flexible use of spatial representations after anterior thalamic lesions. Hippocampus 18:996–1007.

Wyss JM, Van Groen T. 1992. Connections between the retrosplenial cortex and the hippocampal formation in the rat: A review. Hippocampus 2:1–11.

Yiu AP, Rashid AJ, Josselyn SA. 2011. Increasing CREB function in the CA1 region of dorsal hippocampus rescues the spatial memory deficits in a mouse model of Alzheimer's disease. Neuropsychopharmacology 36:2169–2186.